Cell Reports, Volume *28*

Supplemental Information

Re-education of Tumor-Associated Macrophages by CXCR2 Blockade Drives Senescence and Tumor Inhibition in Advanced Prostate Cancer

Diletta Di Mitri, Michela Mirenda, Jelena Vasilevska, Arianna Calcinotto, Nicolas Delaleu, Ajinkya Revandkar, Veronica Gil, Gunther Boysen, Marco Losa, Simone Mosole, Emiliano Pasquini, Rocco D'Antuono, Michela Masetti, Elena Zagato, Giovanna Chiorino, Paola Ostano, Andrea Rinaldi, Letizia Gnetti, Mariona Graupera, Ana Raquel Martins Figueiredo Fonseca, Ricardo Pereira Mestre, David Waugh, Simon Barry, Johann De Bono, and Andrea Alimonti

Supplementary Figure 1

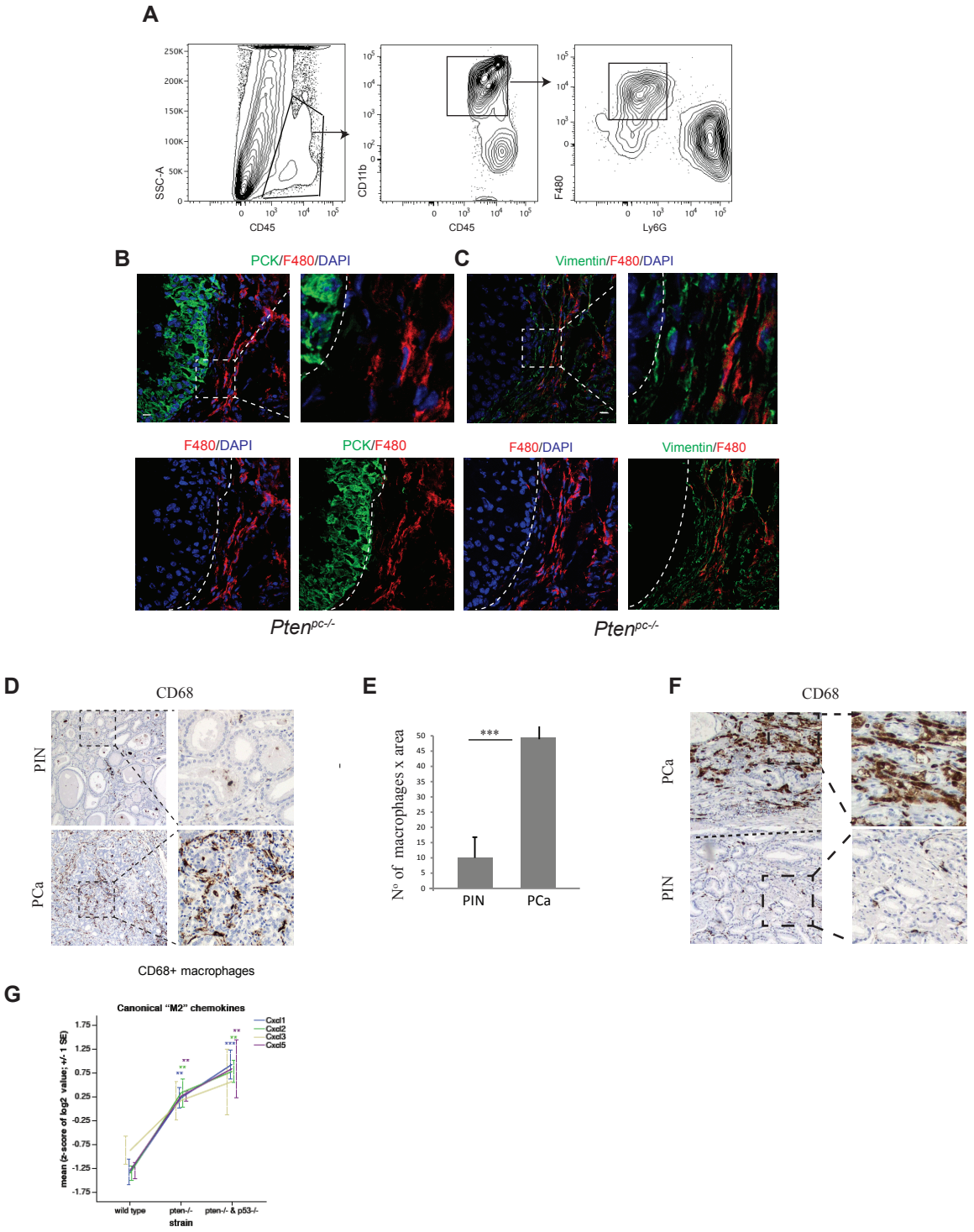

Supplementary Figure 1. TAMs infiltration correlates with tumor progression in murine and human prostatic tumors. Related to Figure 1.

(A) Representative FACS plots of the gating strategy utilized for the characterization and quantification of CD45+CD11b+F480+ TAMs in *Pten*$^{pc-/-}$ and *Pten*$^{pc-/-}$; *Trp53*$^{pc-/-}$ tumors. (B) Representative confocal immunofluorescence images (IF) showing the localization of F4/80^{+} (red) macrophages in *Pten*$^{pc-/-}$ prostatic tumors. Prostatic epithelial tissues are stained with αPan-Cytokeratin (PCK, green). Cells were counterstained with the nuclear marker DAPI (blue). Scale bar: 10 μm (C) Representative confocal immunofluorescence images of F4/80^{+} (red) tumor-infiltrating macrophages and vimentin^{+} cells (green) within anterior prostate lobes from *Pten*$^{pc-/-}$ tumors. Cells were counterstained with the nuclear marker DAPI (blue). Scale bar: 10μm. (D) Representative images and (E) quantification of CD68 IHC staining in adjacent areas of a prostatic tumor, showing TAMs infiltrating in PIN vs PCa areas. Analyses were performed on a human Tissue Microarray (TMA) including N= 10 PIN e N=11 PCa cases. Original magnification 20X. (F) Representative image of a TMA section where PIN and PCa areas co-existed. CD68 staining shows here the preferential infiltration of macrophages in PCa areas. Original magnification 20X. (G) Gene expression levels of CXCL chemokines in tumor tissues from *Pten*$^{pc+/+}$, *Pten*$^{pc-/-}$ and *Pten*$^{pc-/-}$; *Trp53*$^{pc-/-}$ mice, obtained from wild-type mice and prostate cancer models (GSE25140(Ding et al., 2011); probe with highest signal per gene). Group means were compared by computing 1-way Anova with Dunnett's as post-test (SPSS v. 23). Wild-type served as the reference and p-values two-tailed < 0.05 were considered significant. * P<0.05, ** P<0.01, ***P<0.001.

Supplementary Figure 2

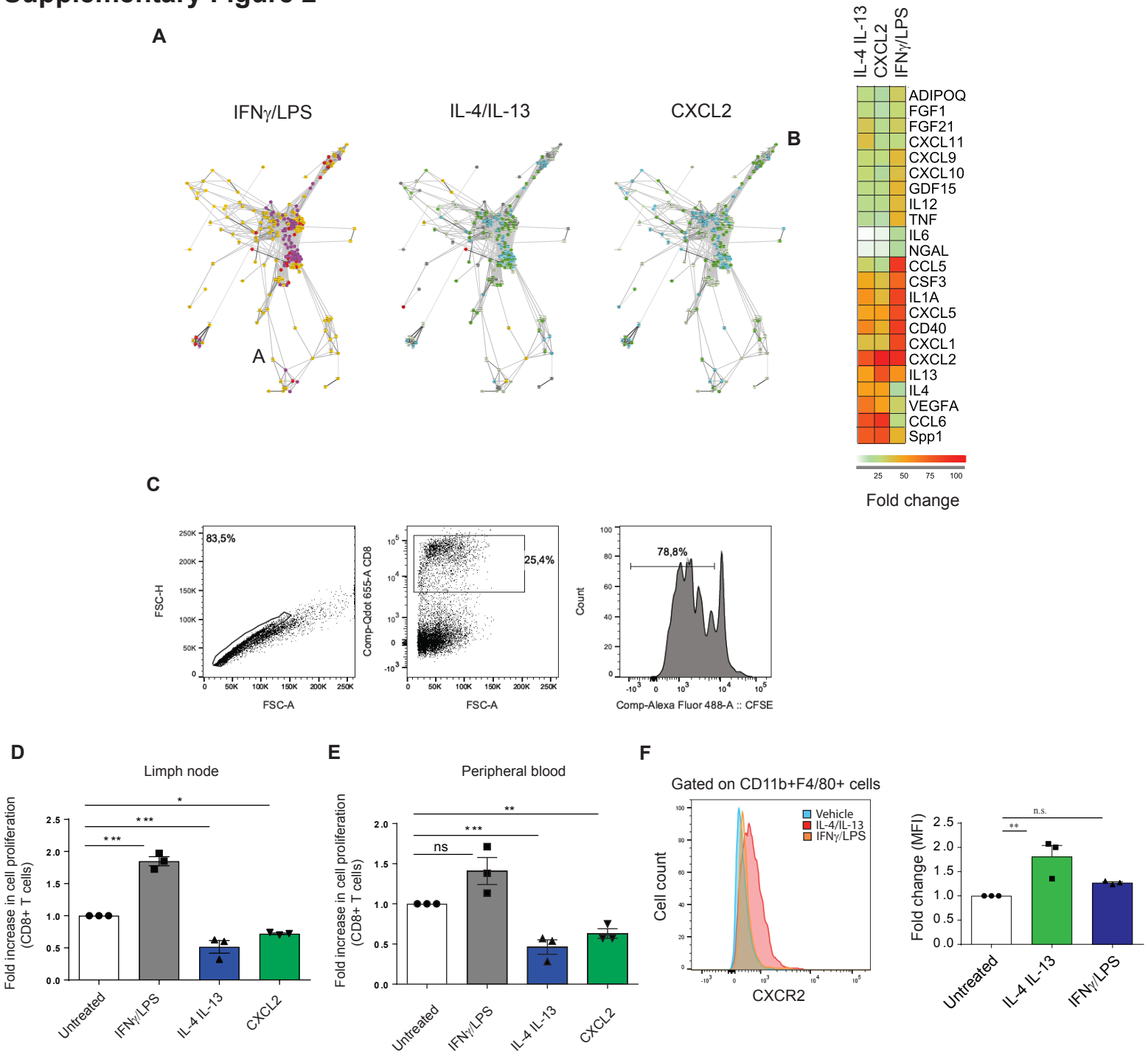

Supplementary Figure 2. Role of the CXCL2-CXCR2 pathway on macrophage polarization *in vitro*. Related to Figure 2. (A) Identification of all gene sets (GSs) pivotal in macrophage polarization with IL-4/IL-13 and IFNγ/LPS from bone marrow-derived macrophage in vitro and their behavior in context with CXCL2-mediated differentiation. Gene set (GSs) enrichment analyses were run on the respective lists (IL-4/IL-13 versus Untreated, CXCL2 versus Untreated and IFNγ/LPS versus Untreated), collapsed for probes yielding the highest signal per gene and ranked for fold-change. 23304 GSs were subjected to analyses of which 8556 were interrogated after filtering for GS-size. GSs enriched in IFNγ/LPS versus untreated and at the same time depleted when comparing IL-4/IL-13 versus untreated or vice versa formed the basic GS-network of pivotal pathways. Network organization is representative of the degree of GS-members connected GSs share (threshold for solid edges ≧ 5%, Cytoscape 3.1.1). For each comparison each node's color denotes significant enrichment (orange = FDRq < 0.05; red = FDRq < 0.01; purple = FDRq < 0.001) or significant depletion (light green = FDRq < 0.05; green = FDRq < 0.01; cyan = FDRq < 0.001) of this GSs. Comparing the three networks, the transcriptional landscape of CXCL2-stimulated macrophages corresponded to 83.6% with IL-4/IL-13 and to 3.8% with IFNγ/LPS. 12.7% of the GSs pivotal to IFNγ/LPS-IL-4/IL-13 differentiation were unaltered following CXCL2 stimulation (node color = grey). (B) Cytokine protein profile of macrophages exposed to IFNγ/LPS, IL-4/IL-13 and CXCL2. Protein profiling was obtained through a cytokine array quantifying 110 proteins (see Methods). Experiment was performed in technical duplicates. (C) Representative FACS plot of the gating strategy utilized for the T cells suppression assay. We analyzed the frequency of CFSE negative (proliferating) cells among $CD8^+$ T lymphocytes. (D,E) Bar graphs showing the quantification of CFSE proliferation assay performed on T cells from (D) Lymph nodes and (E) peripheral blood exposed to macrophages-derived conditioned media in presence or absence of aCXCR2. CSFE negative (proliferating) cells were gated among $CD3^+CD8^+$ cells. (n=3). (F) FACS plot (left panel) and quantification (right panel) showing the frequency of $CXCR2^+$ macrophages upon stimulation with IFNγ/LPS and IL-4/IL-13 in vitro. Mean fluorescence intensity has been measured in CD11b+F480+cells. * P<0.05, ** P<0.01, ***P<0.001.

Supplementary Figure 3

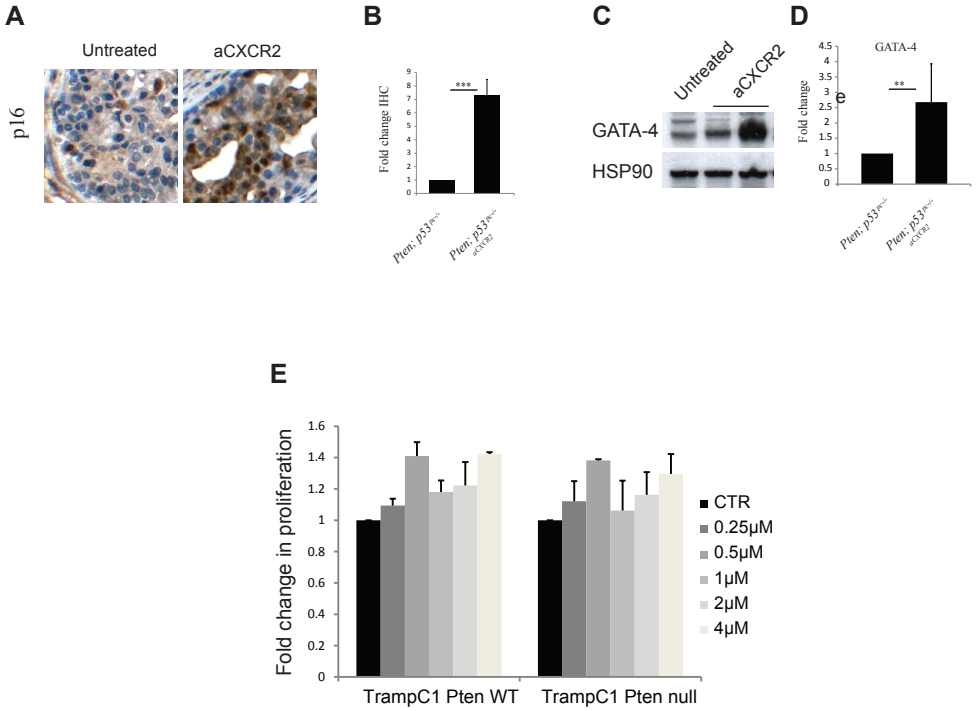

Supplementary Figure 3. TAMs are reprogrammed toward a pro-inflammatory functional state upon treatment with αCXCR2 *in vivo*. Related to Figure 3.

(A) Representative IHC staining (original magnification 20X) and (B) quantification of p16 expression in *Pten*$^{pc-/-}$; *Trp53*$^{pc-/-}$ prostatic tumors upon treatment with αCXCR2 (insert). (C) Western blot analysis and (D) quantification of GATA-4 expression in tumors of mice with or without αCXCR2 treatment. (E) Bar graph showing fold change in proliferation of TRAMP-C1 prostate cancer cells upon exposure to αCXCR2 at different dosages. Cell proliferation was assessed using crystal violet staining. ***P<0.001.

Supplementary Figure 4

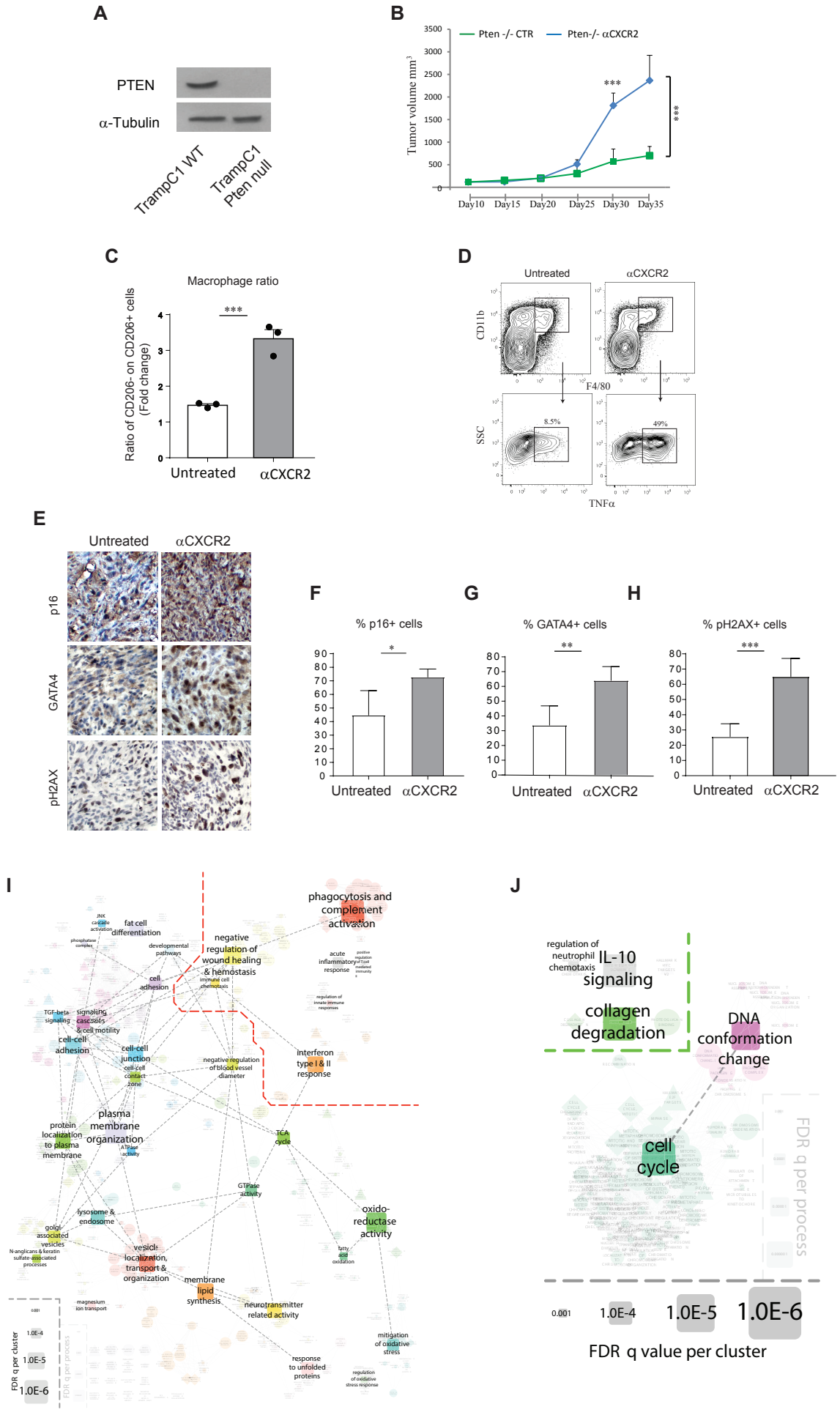

Supplementary Figure 4. αCXCR2 administration reprograms TAMs leading to tumor inhibition in a murine allograft model. Related to Figure 3. (A) Western blot analysis showing *Pten* expression in TRAMP-C1 cells before and after CRISPR/Cas9 mediated deletion. CRISPR/Cas9 was performed on TRAMP-C1 cells to delete *Pten*. (B) Graphs showing the tumor volume of TRAMPC1-*Pten*$^{-/-}$ cells injected subcutaneously, in presence or absence of αCXCR2 treatment. (C) Bar graph from FACS analysis showing the fold change in the ratio between $CD45^{+}CD11b^{+}F4/80^{+}CD11c^{+}CD206^{-}$ and $CD45^{+}CD11b^{+}F4/80^{+}CD11c^{+/-}CD206^{+}$ macrophages infiltrating the TRAMP-C1 allografts. (D) Representative FACS plots of the intracellular staining of TNFα secreted by $CD11b^{+}F4/80^{+}$ tumor infiltrating macrophages upon αCXCR2 treatment. Events are gated on $CD45^{+}$ cells. (E) Representative images of IHC stainings and quantification of (F) p16, (G) GATA4 and (H) pH2AX in TRAMPC1 Pten-/-; Trp53-/- allografts, in presence or absence of the αCXCR2 treatment. Original magnification 20X. (I) Gene set (GS)-cluster network superimposed on the original transcriptional landscape that maps all GSs significantly enriched in FACS sorted TAMs ($CD45^{+}F480^{+}$ cells) after treatment of the tumor bearing mice with the CXCR2 antagonist. The area outlined by the red boarder comprises the significantly upregulated immunity-associated effector processes. For the GS-cluster network superimposed on the GS-GS network: Node color = MCL-cluster; node size = inversely proportional to mean log2 transformed FDRq values of the GSs belonging to this cluster. For the GS-GS network in the background: Node color = MCL-cluster membership; node size = inversely proportional to log2 transformed FDRq values, node shape = database resource; edge color = darker the higher the proportion of leading edge genes overlapping between the nodes it connects is. Data analysis and data visualization for the underlying GS-GS network and the superimposed GS-cluster network were carried out following the methodologies described in detail in the Methods. (J) The area outlined by the green boarder comprises the significantly downregulated immunity-associated effector processes. Underlying analyses, visualization methodology and layout parameters of panel J correspond precisely to the ones listed for panel I. The FDR*q* value reference nodes allow estimation of scaling and direct comparison of the two panels (n=4 samples/group). * $P<0.05$, ** $P<0.01$, *** $P<0.001$.

Supplementary Figure 5

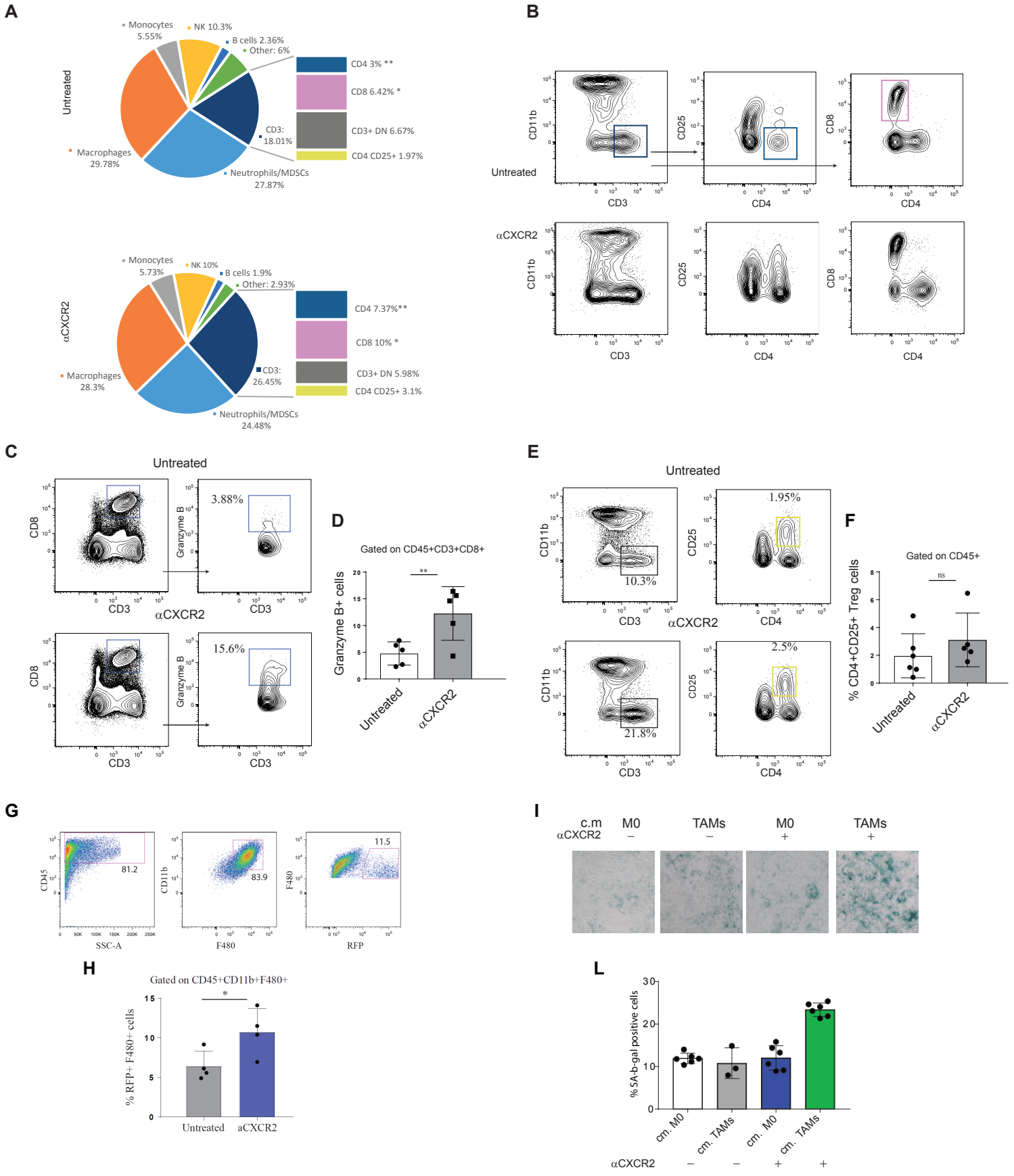

Supplementary Figure 5. ***In vivo*** **αCXCR2 effect on the immune cells infiltrate. Related to Figure 3.**

(A) Pie charts showing percentages of tumor infiltrating immune cells with or without αCXCR2 treatment. Vertical slices on the right of each pie chart represents the different $CD3^+$ subpopulations. Events were gated on $CD45^+$ cells. (n= 5 mice per group) (B) Gating strategy utilized to define $CD4^+$ and $CD8^+$ cells in the untreated (upper panel) and in the αCXCR2 treated mice (lower panel). (C) Representative FACS plots and (D) bar graph showing the percentage of $CD8^+$ Granzyme B^+ T cells that infiltrate the tumor upon aCXCR2 treatment, compared to the untreated tumors. (E) Representative FACS plots and bar graph (F) showing the percentage of $CD4^+$ $CD25^{high}$ T regulatory cells that infiltrate the tumor upon aCXCR2 treatment, compared to the untreated tumors. (G) Representative FACS plots and (H) bar graph showing the percentage of RFP^+ phagocytic macrophages. Events are gated on $CD45^+CD11b^+F4/80^+$cells. (I) Representative images and (J) bar graph showing the quantification of SA-β-galactosidase positive TRAMP-C1 cells exposed to c.m. from macrophages polarized *in vitro* with c.m. from *Pten* $^{-/-}$;Trp53 $^{-/-}$ cells ± αCXCR2. ***P<0.001**, P<0.01, *P<0.05.

Supplementary Figure 6

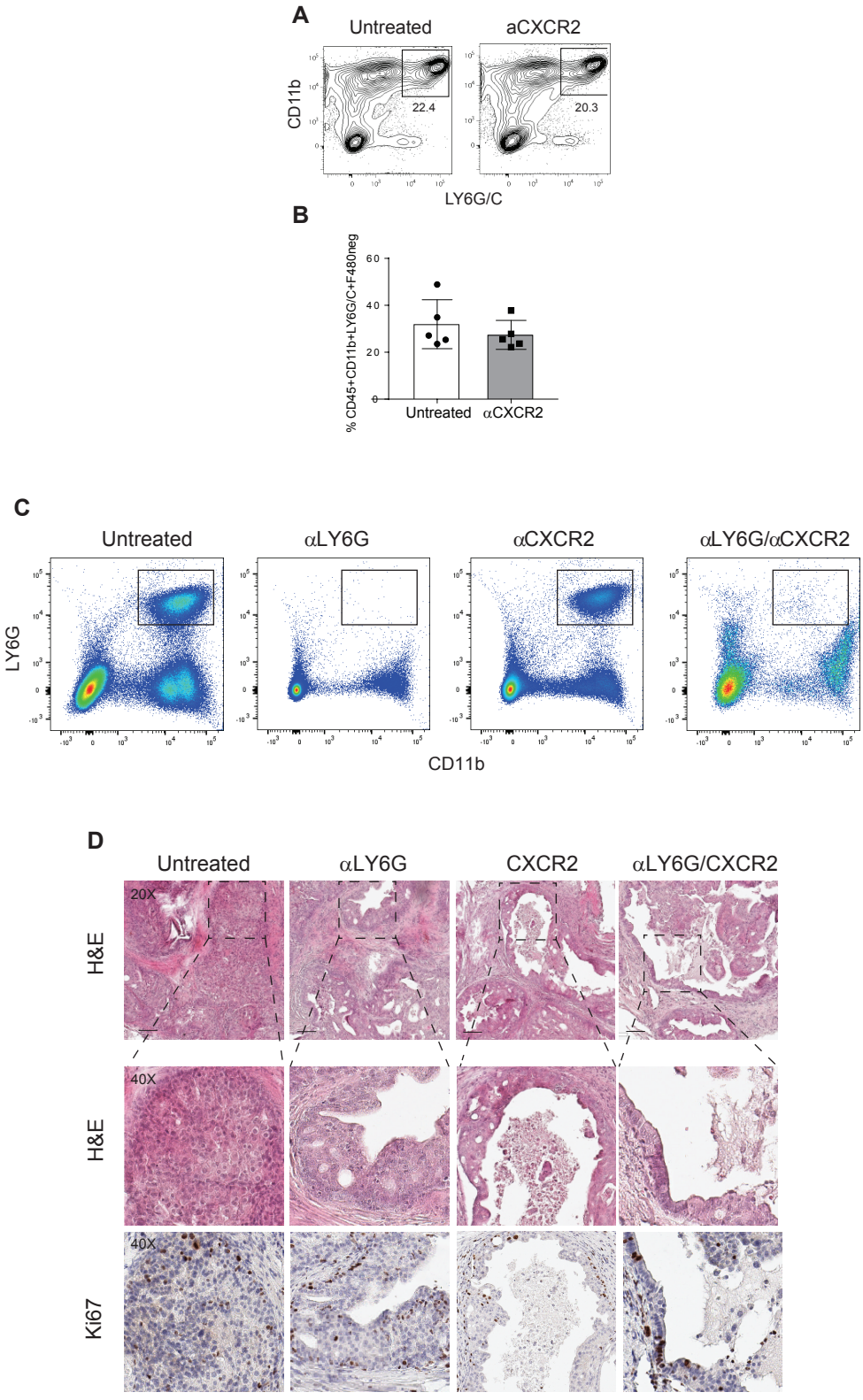

Supplementary Figure 6. ***In vivo*** **αCXCR2 effect on TAMs re-education and tumor inhibition is not affected by Ly6G^{+} cells depletion. Related to Figure 3.**

(A) Representative FACS plots and (B) quantification of the frequency of CD11b^{+} Ly6G/C^{+} tumor infiltrating cells with or without αCXCR2 treatment in *Pten*$^{pc-/-}$; *Trp53*$^{pc-/-}$ mice. Events are gated on CD45^{+} cells. (n=5 mice per group). (C) Representative FACS plots of the frequency of CD11b^{+}Ly6G^{+} circulating cells in peripheral blood and (D) representative images of hematoxylin and eosin (H&E) and Ki67 IHC tumor staining in *Pten*$^{pc-/-}$; *Trp53*$^{pc-/-}$ mice upon daily treatment with 1A8(αLy6G), αCXCR2 or 1A8(αLy6G)/αCXCR2, for 3 weeks. Original magnification 20X. Scalebar: 100μM

Supplementary Figure 7

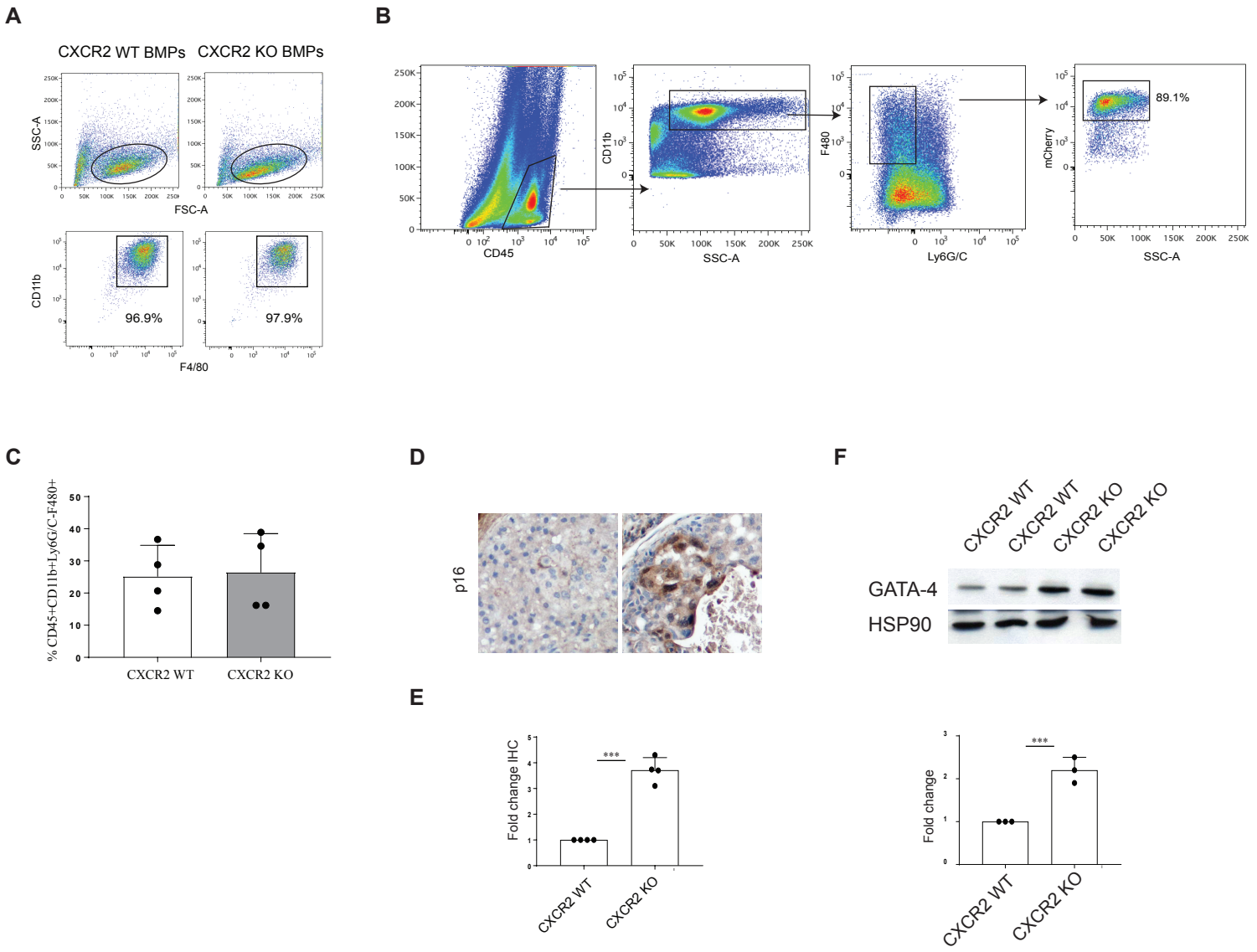

Supplementary Figure 7. Infusion of CXCR2 KO monocytes (vs CXCR2 WT monocytes) in *Pten*$^{pc-/-}$; *Trp53*$^{pc-/-}$ mice drives tumor inhibition and senescence induction. Related to Figure 4.

(A) Representative FACS plots of the gating strategy utilized for the characterization of CXCR2 WT and CXCR2 KO BMDMs after 7 days of *in vitro* differentiation. (B) Representative FACS plots of the gating strategy showing the infiltration of CXCR2 KO UBC-mCherry-labelled monocytes in the tumor after infusion in *Pten*$^{pc-/-}$; *p53*$^{pc-/-}$ mice. *Pten*$^{pc-/-}$; *p53*$^{pc-/-}$ mice were infused with CXCR2 WT or CXCR2 KO monocytes as described in the methods. (C) Bar graph showing the frequency of F4/80^{+} macrophages in tumors of mice infused with CXCR2 WT and CXCR2 KO monocytes. Events are gated in CD45^{+}CD11b^{+} cells. (n= 4 mice per group) (D) Representative images of IHC staining (original magnification 40X) and (E) quantification of western blot analysis of p16 expression in mice upon CXCR2 WT and CXCR2 KO monocytes infusion. (F) Western blot analysis (upper panel) and quantification (lower panel) of GATA-4 expression in tumors after infusion with CXCR2 WT and CXCR2 KO monocytes. ***P<0.001.

Supplementary Figure 8

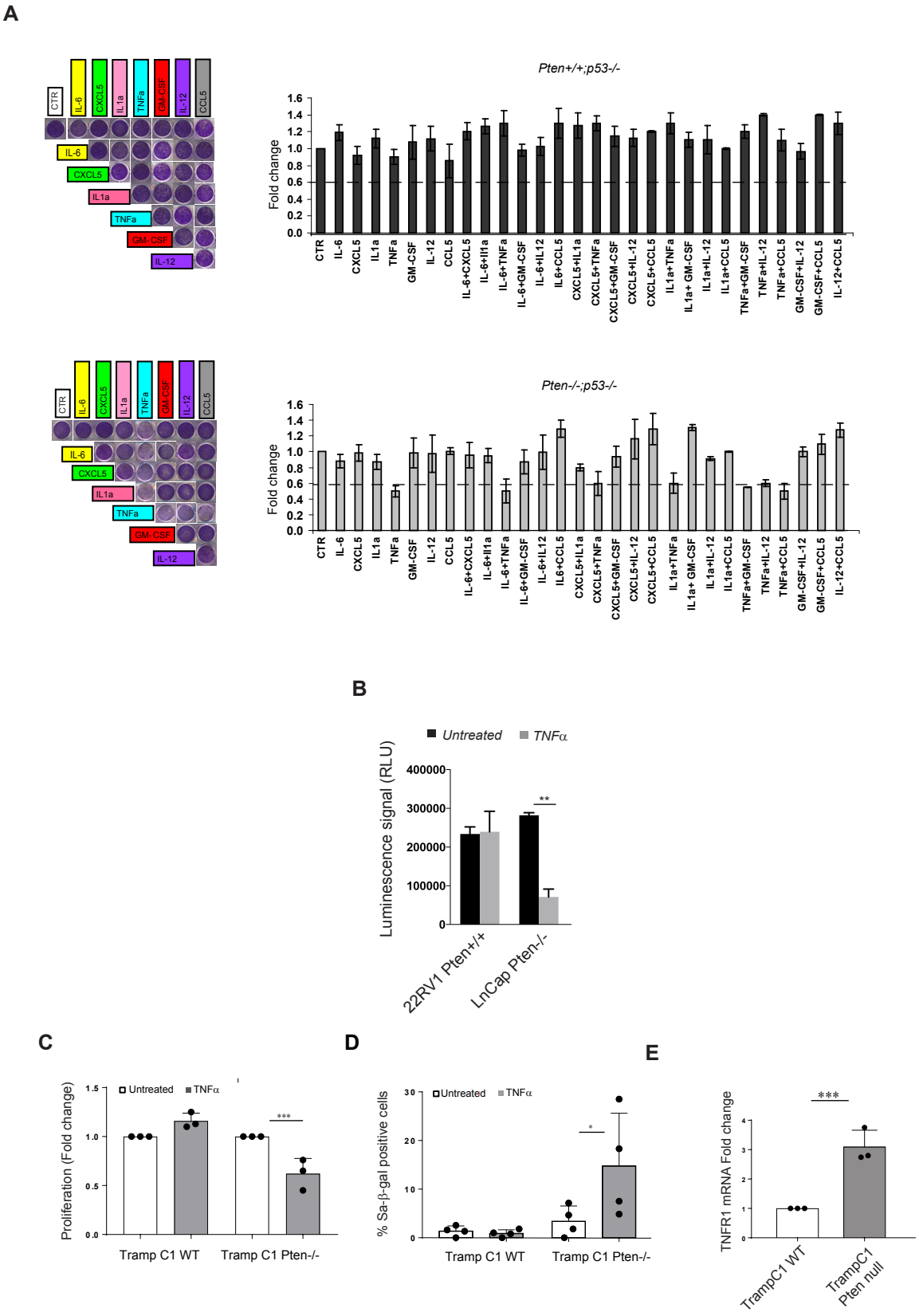

Supplementary Figure 8. *Pten* deletion sensitizes MEFs to TNFα-induced stop of proliferation. Related to Figure 5.

(A) Representative pictures and bar graphs showing the fold change in proliferation of Pten$^{+/+}$; p53$^{-/-}$ (upper panel) and Pten$^{-/-}$, p53$^{-/-}$ MEFs (lower panel) upon exposure to different combinations of cytokines. (B) *In vitro* treatment of 22Rv1 and LNCap cell lines-derived organoids with recombinant TNFα (10 ng/ml). Proliferation was measured by luminescence signal (RLU) after 5 days (C) Bar graph showing the fold change in proliferation of TRAMPC1 Pten$^{+/+}$ and Pten$^{-/-}$ cells exposed to TNFα (10 ng/ml) for 3 days (n=4). (D) Bar graph showing the quantification of SA-β-gal staining on TRAMP-C1 Pten$^{+/+}$ and Pten$^{-/-}$ cells exposed to TNFα for 3 days (n=4). (E) qRT-PCR analysis of *TNFR1* expression in *Pten*$^{+/+}$ and *Pten*$^{-/-}$ TRAMP-C1 cell line (n=3). * P<0.05, ***P<0.001.